THE JOURNAL OF BIOLOGICAL CHEMISTRY VOL. 287, NO. 42, pp. 35612–35620, October 12, 2012

Canonical Transient Receptor Potential (TRPC) 1 Acts as a Negative Regulator for Vanilloid TRPV6-mediated Ca^{2+} Influx*[S]

Received for publication, July 13, 2012, and in revised form, August 24, 2012 Published, JBC Papers in Press, August 29, 2012, DOI 10.1074/jbc.M112.400952

Rainer Schindl[‡1], Reinhard Fritsch[‡], Isaac Jardin[§2], Irene Frischauf[‡3], Heike Kahr[¶], Martin Muik[‡], Maria Christine Riedl[‡], Klaus Groschner[‖], and Christoph Romanin[‡4]

From the [‡]Institute for Biophysics, University of Linz, A-4020 Linz, Austria, the [‖]Institute of Pharmacology and Toxicology, University of Graz, A-8010 Graz, Austria, the [§]Department of Physiology, University of Extremadura, 10003 Caceres, Spain, and the [¶]School of Engineering/Enviromental/Sciences, University of Applied Sciences Upper Austria, A-4600 Wels, Austria

Background: Heteromerization of TRP family members can affect their physiological and biophysical properties.
Results: TRPV6 and TRPC1 associate via their ankyrin-like repeat domains. Co-expression of TRPV6 and TRPC1 reduced TRPV6 expression in the plasma membrane, and hence reduces TRPV6 influx currents.
Conclusion: TRPC1 acts as negative regulator on TRPV6 mediated Ca^{2+} signaling.
Significance: We show here a novel regulation in TRPV6 activity by formation of heterocomplexes with TRPC1.

TRP proteins mostly assemble to homomeric channels but can also heteromerize, preferentially within their subfamilies. The TRPC1 protein is the most versatile member and forms various TRPC channel combinations but also unique channels with the distantly related TRPP2 and TRPV4. We show here a novel cross-family interaction between TRPC1 and TRPV6, a Ca^{2+} selective member of the vanilloid TRP subfamily. TRPV6 exhibited substantial co-localization and *in vivo* interaction with TRPC1 in HEK293 cells, however, no interaction was observed with TRPC3, TRPC4, or TRPC5. Ca^{2+} and Na^{+} currents of TRPV6-overexpressing HEK293 cells are significantly reduced by co-expression of TRPC1, correlating with a dramatically suppressed plasma membrane targeting of TRPV6. In line with their intracellular retention, remaining currents of TRPC1 and TRPV6 co-expression resemble in current-voltage relationship that of TRPV6. Studying the N-terminal ankyrin like repeat domain, structurally similar in the two proteins, we have found that these cytosolic segments were sufficient to mediate a direct heteromeric interaction. Moreover, the inhibitory role of TRPC1 on TRPV6 influx was also maintained by expression of only its N-terminal ankyrin-like repeat domain. Our experiments provide evidence for a functional interaction of TRPC1 with TRPV6 that negatively regulates Ca^{2+} influx in HEK293 cells.

The transient receptor potential (TRP)[5] proteins display a broad tissue expression with a large diversity of cation selectivity, modes of activation and physiological functions (1, 2). All TRP proteins consist of 6 transmembrane domains and assemble into tetramers (3–6). While heterologous expression of TRP proteins predominantly leads to homomeric oligomerization, knock-down strategies have revealed that most native TRPs are aggregated to heteromeric channels that are embedded in larger signaling complexes (7, 8).

Heteromeric TRP channels are well demonstrated within the phospholipase C-coupled TRPC family. TRPCs multimerize within TRPC1/4/5 and TRPC3/6/7 subgroups (9, 10). Only TRPC1 can form heteromers with all other TRPC proteins (11–14) exhibiting a reduced Ca^{2+} permeability compared with the respective homomeric TRPC channel subtype. A novel receptor-dependent ion channel is formed by a heteromer of TRPC1 with the distinctly related polycystic TRPP2 (15–17).

Within the vanilloid TRP channels, TRPV5/6 proteins are not only co-expressed in similar tissues but they can also form heteromeric channels (3, 18). Various heteromeric combinations have been reported within TRPV1 to TRPV4 (20) while Hellwig *et al.* only observed interaction between TRPV1 and TRPV2 (18). Melastatin, mucolipin, and polycycstic TRP include heteromeric channels within their subfamily (5).

Heteromerization between members of TRPC and TRPV subfamilies plays an important role in the regulation of cation influx in a number of tissues. TRPV4 interacts with TRPC1-forming complexes that modulate Ca^{2+} influx in endothelial cells (21). TRPC1 and TRPC6 channels associate with TRPV4 to mediate mechanical hyperalgesia and primary afferent nociceptor sensitization (22). TRPC1 and TRPV6 contributed to Ca^{2+} entry in prostate cells, where TRPV6 expression is shown to be closely related with prostate cancer (23).

* This work was supported by the Austrian Science Foundation (to F. W. F.): Project P22747 (to R. S.), Project P21925 (to K. G.), and Project P18169 as well as P22565 (to C. R.).
⌘ *Author's Choice*—Final version full access.
[S] This article contains supplemental Fig. S1.
[1] To whom correspondence may be addressed: Institute of Biophysics, Johannes Kepler University Linz Gruberstrasse, 40-4020 Linz (Austria). Tel.: +4373224687606; E-mail: rainer.schindl@jku.at.
[2] Supported by MCI fellowship (Ref. BES-2008-002875).
[3] Recipient of a Hertha-Firnberg scholarship (T442).
[4] To whom correspondence may be addressed: Institute of Biophysics, Johannes Kepler University Linz Gruberstrasse, 40-4020 Linz (Austria). E-mail: christoph.romanin@jku.at.

[5] The abbreviations used are: TRP, transient receptor potential; FRET, Förster resonance energy transfer; TRPC, canonical TRP; TRPV6, vanilloid TRP 6; SOCE, store-operated calcium entry; DVF, divalent-free.

Because of its huge variety, the formation of these homo- and heterocomplexes in the TRP family may involve different protein motifs. Homomeric TRPC1 assembly is dependent on an N-terminal coiled-coil region (24), while TRPM2, TRPM8, and TRPP2 use C-terminal coiled-coils for tetramerization (25–30). Instead, TRPC4 and TRPC5 (31), TRPV4 (32), TRPV5, and TRPV6 (33–35) require the ankyrin-like repeats for homo- as well as heteromeric channel assembly. In addition to the ankyrin like repeats, TRPC channels require a C-terminal segment as well (36). Interestingly, TRPC1 seems to use different domains for homo- and heteromerization, and oligomerizes with TRPC3 via their ankyrins (12).

In the present study, we report a novel interaction of TRPC1 and TRPV6 via their ankyrin-like repeats, which down-regulates both TRPV6 expression in the plasma membrane and TRPV6 Ca^{2+} current. The observed down-regulation of TRPV6 currents by TRPC1 may increase the cellular diversity to fine-tune Ca^{2+} homeostasis.

EXPERIMENTAL PROCEDURES

Cell Culture and Molecular Cloning—Human embryonic kidney 293 (HEK293) cells were cultured in DMEM supplemented with L-glutamine (2 mM), streptomycin (100 μg/ml), penicillin (100 units/ml), and 10% fetal calf serum at 37 °C in a humidity-controlled incubator with 7% CO_2. HEK293 cells were transfected with 4 μl of Transfectin (Bio-Rad) and 1 μg of DNA of CFP/YFP-TRPC1 (GenBank™ accession number: NM_003304.4), TRPC3 (U47050), TRPC4 (NM_016984.1), TRPC5 (NM_009428), TRPV6 (AF160798) or fragments. Internal restriction sites were used to generate TRPC1 fragments, TRPV6 constructs have been previously described (37).

Förster Resonance Energy Transfer (FRET) Microscopy—Transfected HEK293 cells grown on cover slips for 1–2 days were transferred to a standard bath solution, including (in mM): 140 NaCl, 5 KCl, 1 $MgCl_2$, 2 $CaCl_2$, 10 glucose, 10 Hepes, pH 7.4 (NaOH).

A QLC100 Real-Time Confocal System (Visitron Systems GmBH, Germany) was used for recording fluorescence images connected to a dual port adapter (dichroic: 505lp; emission 1: 485/30; emission 2: 535/50; Chroma Technology Corp.) and two Photometrics CoolSNAPHQ monochrome cameras (Roper Scientific). This system was attached to an Axiovert 200 M microscope (Zeiss, Germany) and used in conjunction with an argon ion multi-wavelength (454–514 nm) laser (Spectra Physics). The wavelengths were selected by an Acousto Optical Tuneable Filter (VisiTech Int.). MetaMorph 5.0 software (Universal Imaging Corp.) was used to acquire images and to control the confocal system. Illumination times for CFP/FRET and YFP images that were recorded with a minimum delay consecutively of 900 ms. The images were analyzed for FRET using a self-written MatLab 7 programs (37) where the algorithm proposed by Xia (52) was implemented. In short, the recorded FRET image (ex: 457 nm, em 535/50) was corrected for crosstalk from the other imaging channels. The appropriate crosstalk calibration factors were determined for all the constructs used in separate experiments on the days the experiments were done.

Electrophysiology—Electrophysiological experiments were performed at 20–24 °C, using the patch-clamp technique (38) in the whole-cell recording configuration one or 2 days after transfection. Voltage ramps were usually applied every 5s from a holding potential of +70 mV, covering a range of −90 to 90 mV over 200 ms. In all recordings that were performed in divalent-free (DVF) solutions, a 100 ms ramp (−90 mV to +90 mV) was applied every 2 s from a holding potential of 0 mV. Pipette solution was used to decrease cytosolic Ca^{2+} levels containing (in mM) 145 Cs methane sulfonate, 8 NaCl, 5 $MgCl_2$, 10 HEPES, 10 EGTA, pH 7.2. For carbachol and thapsigargin-stimulated HEK293 cells overexpressing TRPC1 or TRPC1/TRPC5, pipette solution was adjusted to 100 nM cytosolic Ca^{2+} by addition of 4.3 $CaCl_2$. Extracellular solution for Ca^{2+} currents consisted of 145 NaCl (or 145 TEA-Cl), 5 CsCl, 1 $MgCl_2$, 10 HEPES, 10 glucose, 10 $CaCl_2$, pH 7.4. DVF solution contained 165 NaCl, 5 CsCl, 10 HEPES, 10 glucose, 10 EDTA, pH 7.4/CsOH. A liquid junction correction of +12 mV resulted from a Cl^--based bath solution and a sulfonate-based pipette solution.

Biotinylation of Cell Surface Membrane Proteins—HEK293 cells were transfected with YFP-TRPV6 or with GFP-TRPV6 and TRPC1. After 24–72 h, cell surface proteins were biotinylated for 30 min at 4 °C using sulfo-NHS-LC-LC-biotin or sulfo-NHS-SS-biotin (0.5 mg/ml; Pierce) as described previously (39). Briefly, cells were incubated 1h at 4 °C with the biotinylation agent. After incubation, 100 mM Tris was added to stop the reaction. Cells were washed twice with PBS to remove excess biotinylation agent and lysed with lysis buffer, pH 8.0, containing 100 mM NaCl, 20 mM Tris, 2 mM EDTA, 10% glycerol, 0.5% Nonidet P40, and supplemented by 20 μl/ml protease inhibitor mixture (Roche Applied Science). Lysed samples were centrifuged at 14,000 × *g* for 15 min. Finally, biotinylated proteins in the supernatant were precipitated using High Capacity Streptavidin Agarose Resin (Pierce) overnight at 4 °C on a rocking platform. The samples were resolved by 10% SDS-PAGE, and protein detection was done as described in Ref. 39. Anti-β-actin (A5441; Sigma) was used to normalize protein expression.

Immunoprecipitation and Immunoblots—Immunoprecipitation and Western blotting were performed as described previously (40). Briefly, 500-μl aliquots of HEK293 suspension (2×10^5 cell/ml) were lysed with an equal volume of lysis buffer, pH 8.0, containing 200 mM NaCl, 40 mM Tris, 4 mM EDTA, 20% glycerol, 1% Nonidet P40, and supplemented by 20 μl/ml protease inhibitor mixture (Roche Applied Science). Aliquots of HEK293 lysates (1 ml) were immunoprecipitated by incubation with 2 μg of either anti-GFP (Sigma-Aldrich) or anti-TRPC1 antibody (Alomone) and 25 μl of protein A-agarose overnight at 4 °C on a rocking platform. The immunoprecipitates were resolved by 10% SDS-PAGE and separated proteins were electrophoretically transferred onto nitrocellulose membranes for subsequent probing. Blots were incubated 1 h with 10% (w/v) BSA in tris-buffered saline with 0.1% Tween 20 (TBST) to block residual protein binding sites. Immunodetection of hTRPV6 and hTRPC1 was achieved using the anti-GFP antibody diluted 1:1000 in TBST or the anti-hTRPC1 antibody diluted 1:250 in TBST overnight, respectively. The primary antibody was removed, and blots were washed six times for 5 min each with TBST. To detect the primary antibody, blots were incubated for 1 h with horseradish peroxidase-conjugated rabbit anti-mouse IgG antibody or horseradish peroxidase-conjugated goat anti-

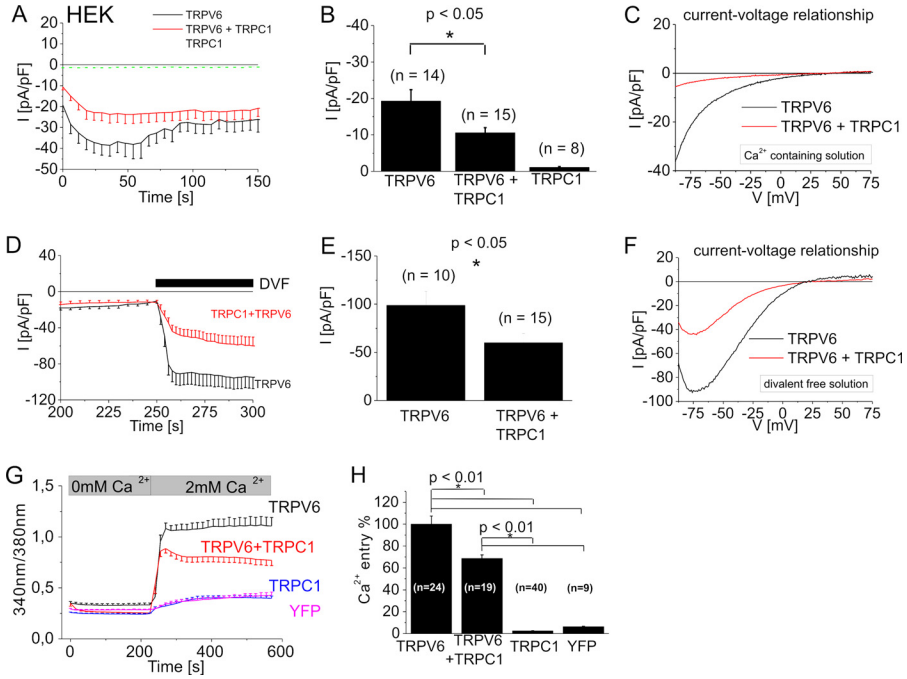

FIGURE 1. **Co-expression of TRPC1 and TRPV6 significantly suppressed TRPV6 currents and Ca^{2+} entry.** Time course of whole-cell voltage ramps (*A*) and statistics on initial currents (*B*) for CFP-TRPC1 and/or YFP-TRPV6 overexpressing HEK293 cells were recorded at −86 mV during voltage ramps with a 10 mM Ca^{2+} bath-solution. Representative current-voltage relationship (*C*) is shown for either TRPV6 or co-expression of TRPC1 and TRPV6. In a DVF solution, co-expression of TRPC1 and TRPV6 in comparison to TRPV6 alone is depicted in the time course (*D*), statistical analysis for current maxima (*E*) and current-voltage relationship (*F*). Intracellular $[Ca^{2+}]_i$ of Fura-2-loaded cells (*G*) was monitored in the time course in a nominally Ca^{2+}-free solution followed by addition of 2 mM Ca^{2+}. Ca^{2+} entry in cells overexpressing TRPV6 and/or TRPC1 or YFP is shown in the time course (*G*) or maximum Ca^{2+} entry (*H*).

rabbit IgG antibody diluted 1:10,000 in TBST and then exposed to enhanced chemiluminiscence reagents for 5 min. Blots were then exposed to photographic films. The density of bands on the film was measured using scanning densitometry. Data were normalized to the amount of protein recovered by the antibody used for the immunoprecipitation.

To determine the amount of TRPC1 that is expressed both in the plasma membrane and in the cytosolic fraction, we performed a double immunoprecipitation using the anti hTRPC1 antibody, directed toward the sequence 557–571 of human hTRPC1, which is located in the pore-forming region between the fifth transmembrane domain and region VII of hTRPC1 (41). Cells with overexpressed, untagged TRPC1 were stimulated with 100 μM CCH for 60 s before mixing with paraformaldehyde (1.5% in PBS). Fixed cells were washed and incubated with 2 μg of anti-TRPC1 (557–571) antibody, which binds an extracellular motif within TRPC1 (11, 42, 43), for 2 h, washed, and lysed. Immunoprecipitation was performed for 2 further hours in the presence of agarose beads and in the absence of anti-TRPC1 antibody. The beads were precipitated by centrifugation, washed, and suspended in loading buffer. The supernatant, containing the TRPC1 cytosolic fraction, was immunoprecipitated overnight with 2 μg of TRPC1 and agarose beads. Both fractions were resolved in a SDS-GEL, and the Western blot was performed using the anti-TRPC1 antibody.

Fura-2 Microscopy—HEK293 cells were grown on coverslips for 2 days and loaded with Fura-2/AM (1 μM) for 30 min at 20 °C in Dulbecco's modified Eagle's medium, washed for three times and dyes were allowed to deesterify for 15 min at 20 °C. Coverslips were transferred to an extracellular solution (see "FRET microscopy") without Ca^{2+} and mounted at an inverted Axiovert 100 TV microscope (Zeiss, Germany). Excitation of Fura-2 was performed at 340 nm and 380 nm, and Ca^{2+} measurements are shown as 340/380 ratios of both YFP and untransfected HEK293 cells.

Statistical Analysis—Data are expressed as means ± S.E., and statistical analysis using Student's *t* test with Origin software (OriginLab, Northampton, MA). Differences are considered significant when *p* values are <0.05.

RESULTS

TRPV6 Currents Are Significantly Suppressed by TRPC1 Co-expression—The TRPC1 protein is the most versatile heteromerization partner of the TRP channels, hence we examined for its impact on the Ca^{2+}-selective TRPV6 channel. We performed whole-cell patch-clamp experiments using a 10 mM Ca^{2+} containing extracellular solution to address the current characteristics of homo- and potentially heteromeric channels. Recordings of yellow fluorescent protein (YFP)-tagged TRPV6 expressing HEK293 cells yielded constitutively active inward currents. Their time courses were monitored at −86 mV by applying repetitive voltage ramps (Fig. 1*A*). TRPV6 currents transiently increased by using a holding potential of +70 mV, followed by a Ca^{2+}/calmodulin-dependent inactivation (33, 37). We analyzed break-in currents immediately after obtaining whole cell configuration for statistical comparison, to avoid Ca^{2+}-dependent modulation (Fig. 1*B*). Larger maximum TRPV6 currents resulted in a more dominant inactivation (data not shown). In contrast, heterologously expressed TRPC1 tagged with cyan fluorescent protein (CFP) did not generate significant current activity (Fig. 1*A*). Co-expression of TRPC1 and TRPV6 led to a similar inwardly rectifying current-voltage

relationship with a reversal potential of >+30 mV as observed with TRPV6 alone (Fig. 1*C*), yet with significantly down-regulated initial currents (Fig. 1*B*). For all experiments, cells with a similar TRPV6 expression (based on fluorescence) were chosen. When extracellular Ca^{2+} solution was exchanged by a divalent-free solution, TRPV6 currents were enhanced, reversed at +16 ± 5 mV (n = 10) and exhibited a typical negative slope at negative potentials in the current voltage relationship (44, 45). A similar current-voltage relationship remained also for the co-expression of TRPC1 and TRPV6 channels with a reversal potential of +17 ± 2 mV (n = 14), although again with significantly reduced inward-currents (Fig. 1, *D--F*). These experiments demonstrate that two typical TRPV6 current-voltage characteristics are fully retained, when TRPV6 was expressed alone or together with TRPC1. TRPC proteins typically yield less selective Ca^{2+} currents and TRPC1 decreases Ca^{2+} selectivity in heteromeric TRPC channels, in comparison to a respective homomeric TRPC channel (2, 14). Hence a heteromeric TRPCV6/TRPC1 channel might lead to an altered TRPV6 IV relationship, which was clearly not the case.

Additionally we utilized Fura-2 microscopy to investigate Ca^{2+} entry of HEK293 cells overexpressing TRPC1 and/or TRPV6. Fura-2-loaded HEK293 cells were initially bathed in a Ca^{2+} free solution. Addition of 2 mM Ca^{2+} resulted in a robust Ca^{2+} entry (Fig. 1*G*) for TRPV6 expressing cells, whereas TRPC1 overexpression led only to a very small Ca^{2+} entry, that was in a similar range as YFP-transfected cells (Fig. 1*G*). Co-expression of TRPC1 and TRPV6 again resulted in an about 30% reduction of Ca^{2+} entry in comparison to TRPV6 alone (Fig. 1, *G* and *H*), consistent with our electrophysiological approach.

Cytosolic TRPC1 Is Relocated to the Plasma Membrane in TRPC1/TRPC5 Heteromers—In our standard conditions, we observed no TRPC1 activity; hence we aimed to stimulate whole-cell currents of TRPC1-overexpressing cells by receptor stimulation or an alternative store depletion. Yet no clear activation was observed upon an application of the physiological agonist carbachol (100 μM; supplemental Fig. S1*A*), or thapsigargin (TG; 1 μM; supplemental Fig. S1*C*), an inhibitor of the Ca^{2+}-ATPase pump in the endoplasmic reticulum that is widely used to study store-operated calcium entry (SOCE) in line with previous results (9, 46). In Fura-2 microscopy experiments, overexpressed TRPC1 failed to exhibit an enhanced Ca^{2+} entry in comparison to a mock control by either carbachol (100 μM, supplemental Fig. S1*D*) or thapsigargin (1 μM, supplemental Fig. S1*E*). Instead, carbachol-activated TRPC5-expressing HEK293 cells yielded an inward-rectifying current-voltage relationship (supplemental Fig. S1, *A* and *B*). A co-expression of TRPC1 and TRPC5 yielded carbachol-sensitive currents with a reduced inward as well as enhanced outward current suggesting a heteromic TRPC1/C5 channel (supplemental Fig. S1, *A* and *B*) (9, 14). As TRPC1 has been shown to mediate carbachol-dependent currents (47), we analyzed whether under our conditions overexpressed TRPC1 might be retained intracellularly in HEK293 cells as previously reported (8, 48). Confocal microscopy revealed a cytosolic localization of overexpressed TRPC1 (supplemental Fig. S1*F* and Fig. 2*D*). In contrast co-expressed TRPC1 and TRPC5 exhibited co-localization (supplemental Fig. S1*G*), with a partial but clear plasma membrane staining of both TRPC proteins.

Reduced Plasma Membrane Localization of TRPV6 Protein by Co-expression with TRPC1—A possible interpretation of suppressed TRPV6 Ca^{2+} entry/current is that co-expression of TRPC1 reduces the plasma membrane localization of TRPV6. Therefore, we quantitatively compared plasma membrane levels of TRPV6 in cells co-expressing TRPV6 and TRPC1 with those exclusively expressing TRPV6 using surface biotinylation. When TRPV6 is expressed alone in HEK293, the channel is partially located in the plasma membrane in resting cells. When YFP-TRPV6 and an untagged TRPC1 were coexpressed, the amount of TRPV6 in the plasma membrane was reduced, compared with those cells that expressed the TRPV6 protein alone (control TRPV6: 23522 ± 1916 *versus* control TRPV6 & TRPC1: 4245 ± 411; n = 5; Fig. 2*A*, *top panel*). To exclude that the reduced expression of TRPV6 in the plasma membrane was due to diminished overall expression of TRPV6 in the cell, we analyzed the total amount of TRPV6 in HEK293 cells either overexpressing TRPV6 alone or together with TRPC1 by Western blot. The obtained data demonstrate that co-expression of TRPC1 together with TRPV6 did not alter the total expression of TRPV6 in HEK293 cells (control TRPV6: 32537 ± 1916 *versus* control TRPV6 & TRPC1: 31245 ± 411; n = 5; Fig. 2*B*, *top panel*). Western blotting of the same membranes with the anti β-actin antibody was used for normalization (Fig. 2, *A* and *B*; *bottom panel*). To determine the amount of TRPC1 that is expressed both in the plasma membrane and in the cytosolic fraction, untagged TRPC1 overexpressed cells were stimulated with 100 μM CCH for 60 s, fixed and the TRPC1 fractions were isolated performing a double immunoprecipitation as described under "Experimental Procedures." Under our conditions we did not detect overexpressed TRPC1 in the plasma membrane fraction either in resting or carbachol (CCH)-stimulated HEK293 cells (Fig. 2*C*). By contrast, the cytosolic fraction showed a clear expression of TRPC1 (Fig. 2*C*). Alternatively we monitored the cellular localization of overexpressed TRPC1 in comparison to TRPV6-expressing cells and their co-expression by confocal microscopy. While TRPC1 remained intracellularly, better visible in an amplified region near the plasma membrane (Fig. 2*D*), TRPV6 exhibited a clustered localization with partial plasma membrane localization (Fig. 2*D*). Upon co-expression of TRPC1 and TRPV6 both proteins exhibited a substantial co-localization, while the plasma membrane expression of TRPV6 was clearly reduced (Fig. 2*E*). Together, these results suggest that TRPC1 is able to suppress TRPV6 dependent currents/entry because of a reduction of TRPV6 plasma membrane expression.

In Vivo Interaction of TRPC1 and TRPV6—It has been described that some members of the TRPC and TRPV families interact and their association may mediate Ca^{2+} influx in endothelial cells (21). We have used confocal Förster Resonance Energy Transfer (FRET) to examine a possible interaction of various TRPC proteins with TRPV6 in a living HEK293 cell. Co-expression of N-terminally tagged CFP-TRPC1 (Fig. 3*A*, *image 2*) or YFP-TRPV6 (Fig. 3*A*, *image 3*), respectively, revealed substantial intracellular co-localization (Fig. 3*A*, *image 4*), similar as TRPC1 overexpression alone (Fig. 3*A*, *image 1*). A

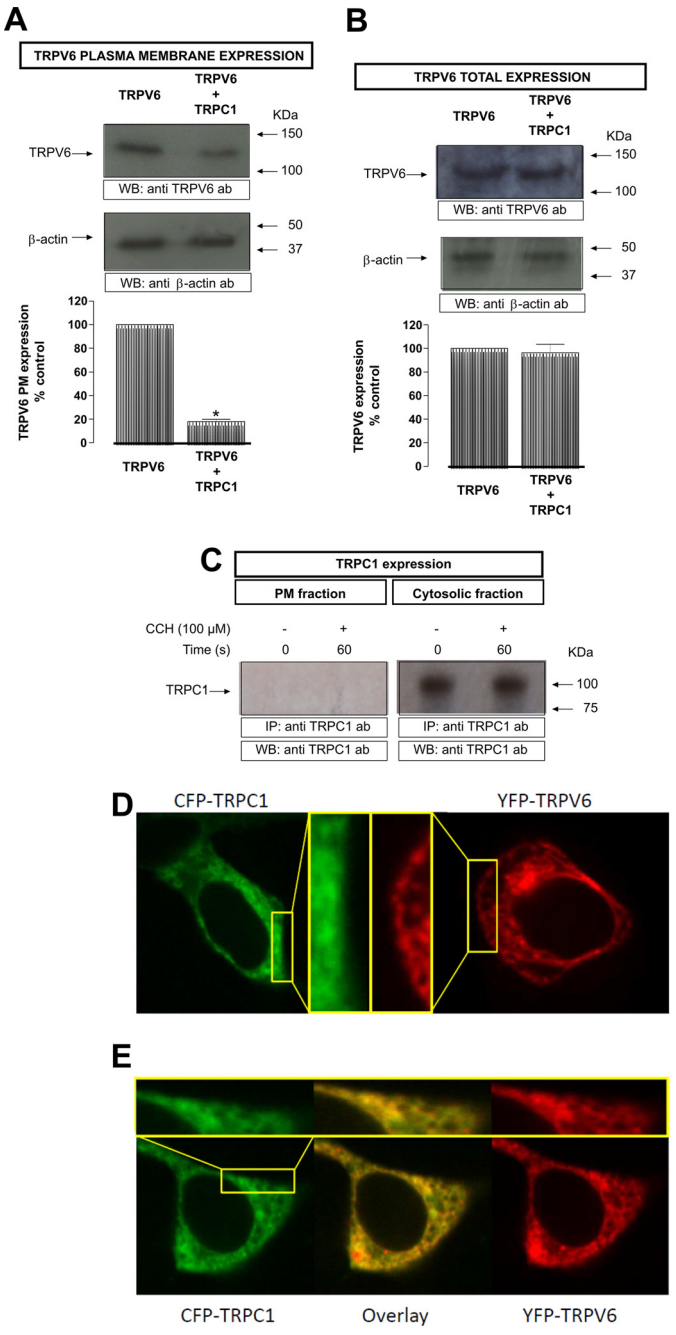

FIGURE 2. **TRPV6 expression in HEK293 cells:** *A*, HEK293 cells, co-expressing either YFP-TRPV6 and/or and TRPC1 were incubated for 1 h at 4 °C with the biotinylation agent. After incubation, 100 mM Tris was added to stop the reaction. Lysed samples were precipitated using streptavidin beads overnight at 4 °C on a rocking platform. *B*, HEK293 cells, co-expressing either TRPV6 or TRPV6 and TRPC1 were lysed. In both cases, the samples were resolved by 10% SDS-PAGE and Western blotting using anti-GFP antibody (*top*). Membranes were re-probed with anti-β-actin antibody (*bottom*). Positions of molecular weight markers are shown on the *right*. These results are representative of five independent experiments. Values are mean ± S.E. *, $p < 0.05$ *versus* resting cells. *C*, HEK293 cells, co-expressing either TRPC1 were stimulated with 100 μM CCH, fixed and the two TRPC1 fractions were isolated by immunoprecipitation. The samples were resolved by 10% SDS-PAGE and Western blotting using anti-TRPC1 antibody. Positions of molecular weight markers are shown on the *right*. These results are representative of six independent experiments. Values are mean ± S.E. *, $p < 0.05$ *versus* resting cells. *D*, localization of a representative CFP-TRPC1 (*left*) as well as YFP-TRPV6 (*right*) transfected HEK293 cell. *E*, localization and overlay of a representative CFP-TRPC1 and YFP-TRPV6 co-expression. The *insets* in *D* and *E* show a higher magnification of a plasma membrane near region.

mean nFRET value of 0.07 suggests a direct coupling of these TRP proteins (Fig. 3, *A*, *image 5* and *F*). Furthermore, we studied the association between TRPV6 and the other members of the TRPC family, to reveal a potential selectivity. In contrast to the predominant intracellular localization of YFP-TRPV6, expression of CFP-TRPC3 mainly targeted to the plasma membrane. Upon their co-expression the plasma membrane staining of TRPC3 was clearly distinct from TRPV6 localization, with minor FRET (Fig. 3*B*). CFP-TRPC4 (Fig. 3*C*) and CFP-TRPC5 (Fig. 3*D*) exhibited a punctate localization in the plasma membrane and vesicular intracellular structures. Both proteins showed partial co-localization with YFP-TRPV6 with small nFRET values (< 0.02; Fig. 3*F*). In comparison to the TRPC1/TRPV6 interaction, average FRET of the homomeric assembly of either CFP-/YFP-TRPC1 (Fig. 3*E*) or previously described CFP-/YFP-TRPV6 (35) are 2-fold increased (Fig. 3*F*). Clearly the TRPC1 isoform exhibited the most pronounced co-localization and highest FRET with TRPV6, in comparison to the other examined TRPC proteins.

Furthermore, to corroborate FRET results we have studied TRPV6-TRPC1 interaction by co-immunoprecipitation. Immunoprecipitation and subsequent SDS-PAGE and Western blotting were conducted using resting HEK293 cells, in the presence of extracellular Ca^{2+}. After immunoprecipitation with anti-TRPC1 antibody, Western blotting revealed the presence of TRPV6. Blotting of the same membranes with the antibody used for immunoprecipitation confirmed similar TRPC1 protein content in all lanes (Fig. 3*G*, *bottom panel*). These data suggest that TRPC1 and TRPV6 proteins are able to assemble within protein complexes and interact with each other when co-expressed in HEK293 cells.

N-terminal Ankyrin-like Repeat Segments of TRPC1 and TRPV6 Interacted Directly—Key domains for functional TRPV6 channel assembly are the six ankyrin-like repeats in the TRPV6 N-terminal strand (33, 35). As TRPC1 also includes three N-terminal ankyrin-like repeats, we focused on these domains as potential interaction sites. Confocal FRET microscopy was used to monitor interaction of CFP-N_{198}-TRPV6, a fragment with four ankyrins that has been previously shown to mediate self-oligomerization (35), with various N-terminal fragments of TRPC1. Co-expression of CFP-N_{198}-TRPV6 (Fig. 4*A*, *1st image*) with YFP-N_{193}-TRPC1 (Fig. 4*A*, *2nd image*) that includes all three ankyrin-like repeats, resulted in cytosolic co-localization (Fig. 4*A*, *3rd image*) and robust FRET (Fig. 4*A*, *4th image*). Average FRET values (Fig. 4*D*) were even stronger than those of the full-length TRPC1-TRPV6 complex (Fig. 3*F*). A dramatically reduced FRET value was calculated for N_{115}-TRPC1 (Fig. 4, *B* and *D*) that included only the first two ankyrin-like repeats or N_{49}-TRPC1 (Fig. 4, *C* and *D*), lacking all ankyrins, when co-expressed with N_{198}-TRPV6. These experiments demonstrate an intrinsic ability of the ankyrin-like repeat domains of TRPC1 and TRPV6 to heteromize *in vivo*.

N-terminal Fragments of TRPC1 that Contain Ankyrin-like Repeats Suppressed TRPV6 Currents—Next, we determined if the ankyrin-mediated interaction is sufficient to down-regulate TRPV6 currents. Co-expression of N_{193}-TRPC1 and TRPV6 indeed significantly reduced TRPV6 currents (Fig. 5*A*), as

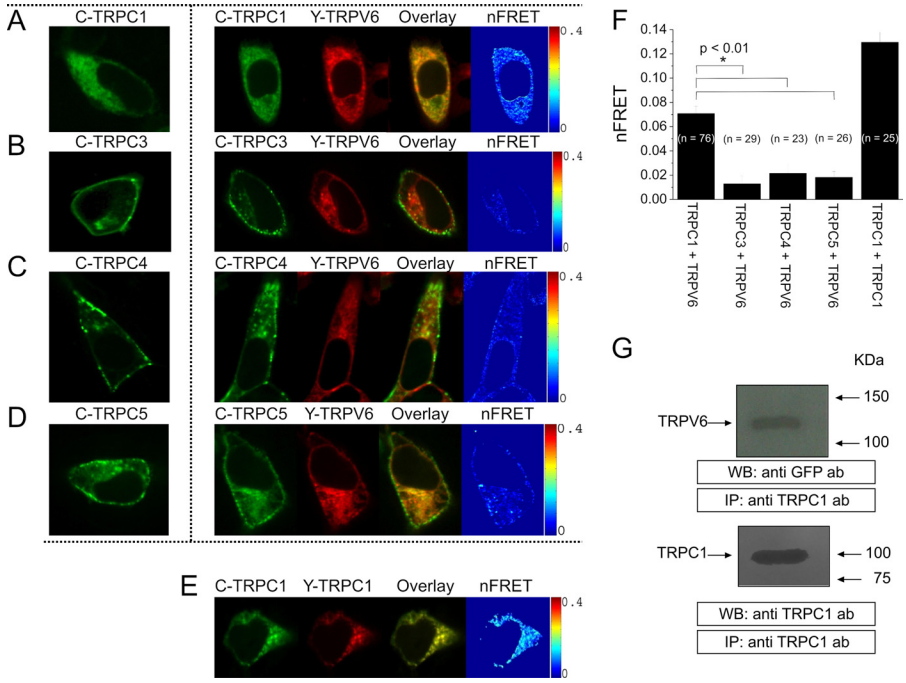

FIGURE 3. **Co-localization and interaction of TRPC1 and TRPV6:** Localization of a representative CFP-TRPC1-expressing cell (*A*, *E*, *image 1*) as well as for a co-expression of CFP-TRPC1 (*A*, *image 2*) with YFP-TRPV6 (*A*, *image 3*), their overlay (*A*, *image 4*) and calculated FRET values (*A*, *image 5*) are presented. Similar image series are shown for co-expression of CFP-TRPC3 (*B*), CFP-TRPC4 (*C*), or CFP-TRPC5 (*D*) with YFP-TRPV6 as well as CFP-/YFP-TRPC1 (*E*). The FRET values depicted in *F* were calculated from the averages of whole cell areas determined from the respective number of cells showing significantly increased FRET values and co-localization of cells co-expressing either CFP-TRPC1 and YFP-TRPV6 (FRET = 0.07 ± 0.01) and CFP-/YFP-TRPC1 (FRET = 0.13 ± 0.01) in contrast to CFP-TRPC3 and YFP-TRPV6 (FRET = 0.01 ± 0.01), CFP-TRPC4 and YFP-TRPV6 (FRET = 0.02 ± 0.01) or CFP-TRPC5 and YFP-TRPV6 (FRET = 0.02 ± 0.01). *G*, HEK293 cells, co-expressing YFP-TRPV6 and TRPC1 were lysed and immunoprecipitated (*IP*) with anti-TRPC1 antibody followed by Western blotting using anti-GFP antibody (*top*). Membranes were reprobed with the immunoprecipitating antibody (*bottom*). Positions of molecular mass markers are shown on the *right*. These results are representative of four independent experiments. Values are mean ± S.E. of four independent experiments. *, $p < 0.05$ *versus* resting cells.

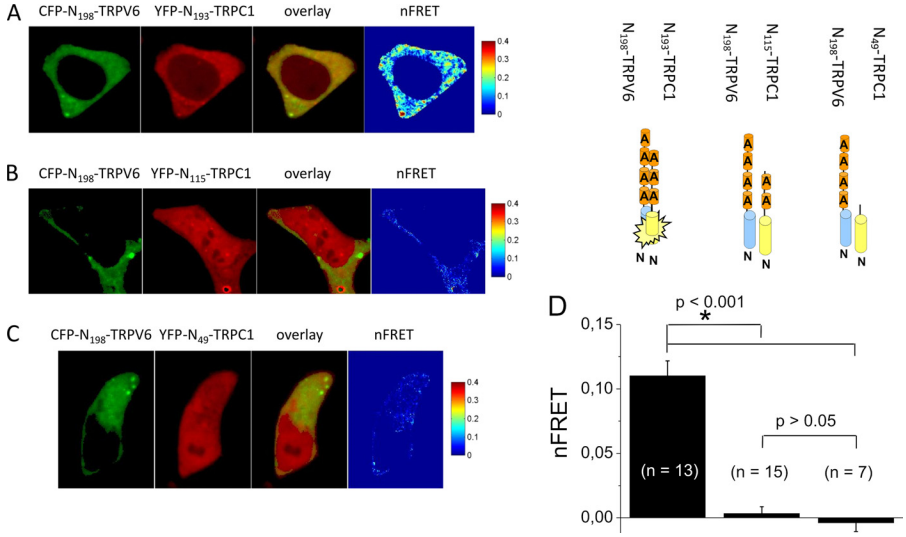

FIGURE 4. ***In vivo* interaction of the ankyrin-like repeat domains of TRPC1 and TRPV6:** Localization of CFP-N_{198}-TRPV6 (*A*, *image 1*) and YFP-N_{193}-TRPC1 (*A*, *image 2*), overlay (*A*, *image 3*), and calculated FRET values (*A*, *image 4*) are presented for a representative HEK293 cell. Similar image series are shown for co-expression of CFP-N_{198}-TRPV6 with YFP-N_{115}-TRPC1 (*B*) or YFP-N_{49}-TRPC1 (*C*). Average FRET values depicted in *D* showed significantly increased FRET values and good co-localization of cells co-expressing CFP-N_{198}-TRPV6 and YFP-N_{193}-TRPC1 (FRET = 0.11 ± 0.01) in contrast to CFP-N_{198}-TRPV6 and YFP-N_{115}-TRPC1 (FRET = 0.00 ± 0.01) or CFP-N_{198}-TRPV6 and YFP-N_{49}-TRPC1 (FRET = 0.00 ± 0.01).

shown in the time courses and statistical analysis on inward currents immediately after whole cell break-in. In contrast, currents of cells co-expressing TRPV6 with ΔN_{193}-TRPC1, a TRPC1 mutant lacking the ankyrin-like repeat domain, (Fig. 5*B*) were not significantly different to those recorded from TRPV6-expressing HEK293 cells. Additionally, N_{115}-TRPC1 (2 ankyrin-like repeats; Fig. 5*C*) or N_{49}-TRPC1 (no ankyrin-like repeats; Fig. 5*D*) failed to significantly reduce TRPV6 currents, in comparison to control TRPV6. None of the TRPC1 fragments affected the inward rectifying current-voltage relationship of TRPV6 (Fig. 5*E*). These experiments suggest that the ankyrin-like repeats mediate an important role in the interac-

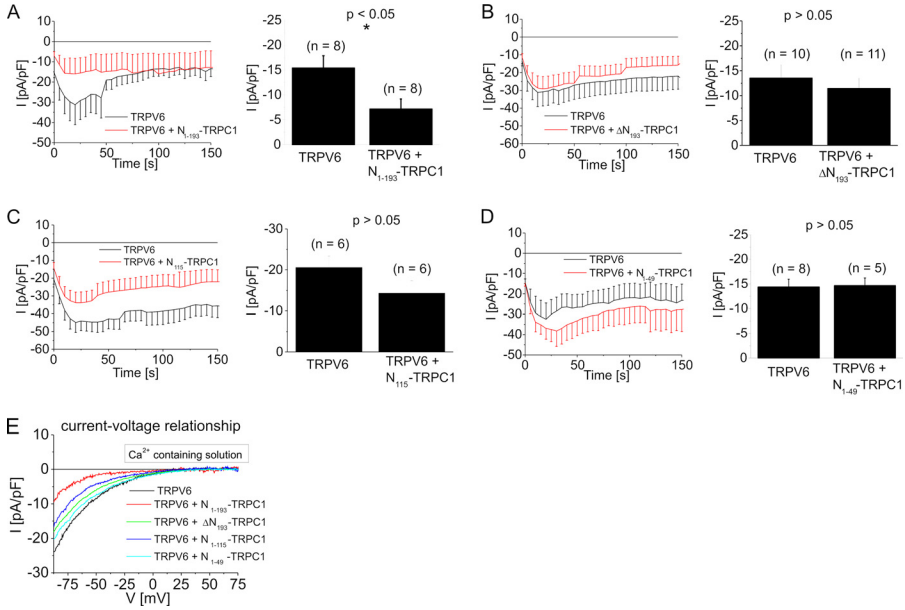

FIGURE 5. **Dominant negative effect of a TRPC1 fragment including the whole ankyrin domain on TRPV6:** Time course and statistics on initial inward currents showed that co-expression of N_{193}-TRPC1 fragment and TRPV6 (*A*) yielded significantly down-regulated currents in comparison to TRPV6-expressing cells. In contrast neither ΔN_{193}-TRPC1 (*B*), TRPC1 lacking all N-terminal ankyrin-like repeats), nor N_{115}-TRPC1 (*C*) or N_{49}-TRPC1 (*D*) were able to suppress co-expressed TRPV6 currents in HEK293 cells. Representative current-voltage relationships (*E*) are shown for experiments shown in *A–D*.

tion of TRPC1 and TRPV6, thereby reducing the amount of plasma membrane-targeted TRPV6.

DISCUSSION

In the present study we identified a specific interaction between TRPC1 and TRPV6 by confocal FRET microscopy and co-immunoprecipitation in HEK293 cells. Heterologous co-expression of TRPC1 and TRPV6 resulted in a strongly diminished plasma membrane expression of TRPV6 corresponding with significantly down-regulated TRPV6-mediated Ca^{2+} entry/currents. The current-voltage relationship of the remaining TRPC1/TRPV6 currents was identical to that of TRPV6 suggesting that this interaction retains TRPV6 in intracellular compartments.

In the small intestine, kidney and bone TRPV6 channel is required for Ca^{2+} influx (49). To tightly control the cytosolic Ca^{2+} levels, TRPV6 expression is adjusted by caliotropic hormones, pH and Ca^{2+}-dependent mechanism (50). In addition, various channel-associated proteins, including S100A10, calmodulin, 80K-H, or Rab11a (50) can regulate TRPV6 activity. Hence, the here discovered TRPC1 and TRPV6 interaction increases the variety of regulatory proteins for Ca^{2+} uptake.

Our biotinylation experiments and confocal images suggested an intracellular retention of TRPV6 by TRPC1 co-expression. Moreover confocal FRET microscopy revealed that an interaction of TRPC1 and TRPV6 already occurred in intracellular compartments. TRPC1 *per se* remained in intracellular compartments in HEK293 cells in line with Ref. 8, 48, hence interaction with TRPV6 interferes with the plasma membrane targeting of the latter. The remaining currents of TRPC1 and TRPV6-co-expressing cells resembled those of TRPV6, suggesting that this current is formed by a fraction of remaining homomeric TRPV6 channels.

Our experiments did not favor a heteromeric channel of TRPC1 and TRPV6 resulting in a decreased channel activity. TRPC1 proteins can clearly contribute to a functional pore in homomeric (47) and heteromeric (9, 13, 14) TRPC channels. However, heteromeric TRPC channels, including TRPC1 with any other TRPC isoform yielded unique permeation properties that could be distinguished from their respective homomeric TRPC channels. Co-expression of TRPC1 and TRPV6 retained the current-voltage profile in a Ca^{2+} and Na^{+} divalent free solution. Hence it is more likely that in a co-expression of TRPC1 and TRPV6, only a remaining TRPV6 channel fraction is targeted to the plasma membrane.

In contrast to TRPC1, co-localization of TRPC3, TRPC4 or TRPC5 with TRPV6 in living HEK293 cells was weak, failed to affect the partial plasma membrane targeting of TRPV6 and yielded very small FRET values. The interaction of TRPC1 and TRPV6 was intrinsically mediated by their N-terminal ankyrin-like repeats. Cytosolic TRPC1/V6 ankyrin segments were sufficient to associate *in vivo* as monitored by confocal FRET microscopy. Consistently, electrophysiological measurements revealed that the ankyrin-like repeats of TRPC1 significantly down-regulated TRPV6 currents, while a TRPC1 mutant lacking these repeats failed to exert a dominant negative effect on TRPV6.

The N-terminal ankyrin-like repeat domain is present in the seven members of canonical TRPCs, the six vanilloid TRPV and TRPA1. Indeed mutations, splice variants or deletion of single ankyrin-like repeats in TRPC5, TRPV5 and TRPV6 disrupted their ability to multimerize (31–34). However, analytical size exclusion chromatography as well as crystallization yielded a monomeric TRPV6 ankyrin-like repeat in solution (19). These *in vitro* studies in comparison to our and other *in vivo* experiments can be reconciled if endogenous factors may facilitate the ankyrin-like repeat assembly.

An important function of TRPV6 is the Ca^{2+} uptake in the small intestine, kidney, and bone (51). Yet a physiological role

and the localization of TRPC1 in these tissues are hampered as long as TRPV6 currents are not functionally identified in native cell systems. Further studies are needed to analyze the physiological consequence of this intrinsic TRPC1-TRPV6 interaction in the small intestine, kidney, and bone.

Acknowledgment—We thank S. Buchegger for excellent technical assistance.

REFERENCES

1. Venkatachalam, K., and Montell, C. (2007) TRP channels. *Annu. Rev. Biochem.* **76,** 387–417
2. Wu, L. J., Sweet, T. B., and Clapham, D. E. (2010) International Union of Basic and Clinical Pharmacology. LXXVI. Current progress in the mammalian TRP ion channel family. *Pharmacol. Rev.* **62,** 381–404
3. Hoenderop, J. G., Voets, T., Hoefs, S., Weidema, F., Prenen, J., Nilius, B., and Bindels, R. J. (2003) Homo- and heterotetrameric architecture of the epithelial Ca^{2+} channels TRPV5 and TRPV6. *EMBO J.* **22,** 776–785
4. Kedei, N., Szabo, T., Lile, J. D., Treanor, J. J., Olah, Z., Iadarola, M. J., and Blumberg, P. M. (2001) Analysis of the native quaternary structure of vanilloid receptor 1. *J. Biol. Chem.* **276,** 28613–28619
5. Cheng, W., Sun, C., and Zheng, J. (2010) Heteromerization of TRP channel subunits: extending functional diversity. *Protein Cell* **1,** 802–810
6. Schindl, R., and Romanin, C. (2007) Assembly domains in TRP channels. *Biochem. Soc. Trans.* **35,** 84–85
7. Freichel, M., Vennekens, R., Olausson, J., Stolz, S., Philipp, S. E., Weissgerber, P., and Flockerzi, V. (2005) Functional role of TRPC proteins in native systems: implications from knockout and knock-down studies. *J. Physiol.* **567,** 59–66
8. Beech, D. J., Xu, S. Z., McHugh, D., and Flemming, R. (2003) TRPC1 store-operated cationic channel subunit. *Cell Calcium* **33,** 433–440
9. Strübing, C., Krapivinsky, G., Krapivinsky, L., and Clapham, D. E. (2001) TRPC1 and TRPC5 form a novel cation channel in mammalian brain. *Neuron* **29,** 645–655
10. Hofmann, T., Schaefer, M., Schultz, G., and Gudermann, T. (2002) Subunit composition of mammalian transient receptor potential channels in living cells. *Proc. Natl. Acad. Sci. U.S.A.* **99,** 7461–7466
11. Jardin, I., Lopez, J. J., Salido, G. M., and Rosado, J. A. (2008) Orai1 mediates the interaction between STIM1 and hTRPC1 and regulates the mode of activation of hTRPC1-forming Ca^{2+} channels. *J. Biol. Chem.* **283,** 25296–25304
12. Liu, X., Bandyopadhyay, B. C., Singh, B. B., Groschner, K., and Ambudkar, I. S. (2005) Molecular analysis of a store-operated and 2-acetyl-*sn*-glycerol-sensitive non-selective cation channel. Heteromeric assembly of TRPC1-TRPC3. *J. Biol. Chem.* **280,** 21600–21606
13. Strübing, C., Krapivinsky, G., Krapivinsky, L., and Clapham, D. E. (2003) Formation of novel TRPC channels by complex subunit interactions in embryonic brain. *J. Biol. Chem.* **278,** 39014–39019
14. Storch, U., Forst, A. L., Philipp, M., Gudermann, T., and Mederos y Schnitzler, M. (2012) Transient receptor potential channel 1 (TRPC1) reduces calcium permeability in heteromeric channel complexes. *J. Biol. Chem.* **287,** 3530–3540
15. Tsiokas, L., Arnould, T., Zhu, C., Kim, E., Walz, G., and Sukhatme, V. P. (1999) Specific association of the gene product of PKD2 with the TRPC1 channel. *Proc. Natl. Acad. Sci. U.S.A.* **96,** 3934–3939
16. Bai, C. X., Giamarchi, A., Rodat-Despoix, L., Padilla, F., Downs, T., Tsiokas, L., and Delmas, P. (2008) Formation of a new receptor-operated channel by heteromeric assembly of TRPP2 and TRPC1 subunits. *EMBO Rep.* **9,** 472–479
17. Kobori, T., Smith, G. D., Sandford, R., and Edwardson, J. M. (2009) The transient receptor potential channels TRPP2 and TRPC1 form a heterotetramer with a 2:2 stoichiometry and an alternating subunit arrangement. *J. Biol. Chem.* **284,** 35507–35513
18. Hellwig, N., Albrecht, N., Harteneck, C., Schultz, G., and Schaefer, M. (2005) Homo- and heteromeric assembly of TRPV channel subunits. *J. Cell Sci.* **118,** 917–928
19. Phelps, C. B., Huang, R. J., Lishko, P. V., Wang, R. R., and Gaudet, R. (2008) Structural analyses of the ankyrin repeat domain of TRPV6 and related TRPV ion channels. *Biochemistry* **47,** 2476–2484
20. Cheng, W., Yang, F., Takanishi, C. L., and Zheng, J. (2007) Thermosensitive TRPV channel subunits coassemble into heteromeric channels with intermediate conductance and gating properties. *J. Gen. Physiol.* **129,** 191–207
21. Ma, X., Qiu, S., Luo, J., Ma, Y., Ngai, C. Y., Shen, B., Wong, C. O., Huang, Y., and Yao, X. (2010) Functional role of vanilloid transient receptor potential 4-canonical transient receptor potential 1 complex in flow-induced Ca2+ influx. *Arterioscler. Thromb. Vasc. Biol.* **30,** 851–858
22. Alessandri-Haber, N., Dina, O. A., Chen, X., and Levine, J. D. (2009) TRPC1 and TRPC6 channels cooperate with TRPV4 to mediate mechanical hyperalgesia and nociceptor sensitization. *J. Neurosci.* **29,** 6217–6228
23. Vanden Abeele, F., Shuba, Y., Roudbaraki, M., Lemonnier, L., Vanoverberghe, K., Mariot, P., Skryma, R., and Prevarskaya, N. (2003) Store-operated Ca^{2+} channels in prostate cancer epithelial cells: function, regulation, and role in carcinogenesis. *Cell Calcium* **33,** 357–373
24. Engelke, M., Friedrich, O., Budde, P., Schäfer, C., Niemann, U., Zitt, C., Jüngling, E., Rocks, O., Lückhoff, A., and Frey, J. (2002) Structural domains required for channel function of the mouse transient receptor potential protein homologue TRP1β. *FEBS Lett.* **523,** 193–199
25. Mei, Z. Z., Xia, R., Beech, D. J., and Jiang, L. H. (2006) Intracellular coiled-coil domain engaged in subunit interaction and assembly of melastatin-related transient receptor potential channel 2. *J. Biol. Chem.* **281,** 38748–38756
26. Mei, Z. Z., and Jiang, L. H. (2009) Requirement for the N-terminal coiled-coil domain for expression and function, but not subunit interaction of, the ADPR-activated TRPM2 channel. *J. Membr. Biol.* **230,** 93–99
27. Tsuruda, P. R., Julius, D., and Minor, D. L., Jr. (2006) Coiled coils direct assembly of a cold-activated TRP channel. *Neuron* **51,** 201–212
28. Hanaoka, K., Qian, F., Boletta, A., Bhunia, A. K., Piontek, K., Tsiokas, L., Sukhatme, V. P., Guggino, W. B., and Germino, G. G. (2000) Co-assembly of polycystin-1 and -2 produces unique cation-permeable currents. *Nature* **408,** 990–994
29. Yu, F., Sun, L., and Machaca, K. (2009) Orai1 internalization and STIM1 clustering inhibition modulate SOCE inactivation during meiosis. *Proc. Natl. Acad. Sci. U.S.A.* **106,** 17401–17406
30. Giamarchi, A., Feng, S., Rodat-Despoix, L., Xu, Y., Bubenshchikova, E., Newby, L. J., Hao, J., Gaudioso, C., Crest, M., Lupas, A. N., Honoré, E., Williamson, M. P., Obara, T., Ong, A. C., and Delmas, P. (2010) A polycystin-2 (TRPP2) dimerization domain essential for the function of heteromeric polycystin complexes. *EMBO J.* **29,** 1176–1191
31. Schindl, R., Frischauf, I., Kahr, H., Fritsch, R., Krenn, M., Derndl, A., Vales, E., Muik, M., Derler, I., Groschner, K., and Romanin, C. (2008) The first ankyrin-like repeat is the minimum indispensable key structure for functional assembly of homo- and heteromeric TRPC4/TRPC5 channels. *Cell Calcium* **43,** 260–269
32. Arniges, M., Fernández-Fernández, J. M., Albrecht, N., Schaefer, M., and Valverde, M. A. (2006) Human TRPV4 channel splice variants revealed a key role of ankyrin domains in multimerization and trafficking. *J. Biol. Chem.* **281,** 1580–1586
33. Erler, I., Hirnet, D., Wissenbach, U., Flockerzi, V., and Niemeyer, B. A. (2004) Ca^{2+}-selective transient receptor potential V channel architecture and function require a specific ankyrin repeat. *J. Biol. Chem.* **279,** 34456–34463
34. Chang, Q., Gyftogianni, E., van de Graaf, S. F., Hoefs, S., Weidema, F. A., Bindels, R. J., and Hoenderop, J. G. (2004) Molecular determinants in TRPV5 channel assembly. *J. Biol. Chem.* **279,** 54304–54311
35. Kahr, H., Schindl, R., Fritsch, R., Heinze, B., Hofbauer, M., Hack, M. E., Mörtelmaier, M. A., Groschner, K., Peng, J. B., Takanaga, H., Hediger, M. A., and Romanin, C. (2004) CaT1 knock-down strategies fail to affect CRAC channels in mucosal-type mast cells. *J. Physiol.* **557,** 121–132
36. Lepage, P. K., and Boulay, G. (2007) Molecular determinants of TRP channel assembly. *Biochem. Soc. Trans.* **35,** 81–83
37. Derler, I., Hofbauer, M., Kahr, H., Fritsch, R., Muik, M., Kepplinger, K., Hack, M. E., Moritz, S., Schindl, R., Groschner, K., and Romanin, C. (2006)

Dynamic but not constitutive association of calmodulin with rat TRPV6 channels enables fine tuning of Ca^{2+}-dependent inactivation. *J. Physiol.* **577,** 31–44
38. Hamill, O. P., Marty, A., Neher, E., Sakmann, B., and Sigworth, F. J. (1981) Improved patch-clamp techniques for high-resolution current recording from cells and cell-free membrane patches. *Pflugers Arch.* **391,** 85–100
39. de Groot, T., van der Hagen, E. A., Verkaart, S., te Boekhorst, V. A., Bindels, R. J., and Hoenderop, J. G. (2011) Role of the transient receptor potential vanilloid 5 (TRPV5) protein N terminus in channel activity, tetramerization, and trafficking. *J. Biol. Chem.* **286,** 32132–32139
40. Jardin, I., Gómez, L. J., Salido, G. M., and Rosado, J. A. (2009) Dynamic interaction of hTRPC6 with the Orai1-STIM1 complex or hTRPC3 mediates its role in capacitative or non-capacitative Ca(2+) entry pathways. *Biochem. J.* **420,** 267–276
41. Wes, P. D., Chevesich, J., Jeromin, A., Rosenberg, C., Stetten, G., and Montell, C. (1995) TRPC1, a human homolog of a *Drosophila* store-operated channel. *Proc. Natl. Acad. Sci. U.S.A.* **92,** 9652–9656
42. Rosado, J. A., Brownlow, S. L., and Sage, S. O. (2002) Endogenously expressed Trp1 is involved in store-mediated Ca^{2+} entry by conformational coupling in human platelets. *J. Biol. Chem.* **277,** 42157–42163
43. Jardín, I., Redondo, P. C., Salido, G. M., and Rosado, J. A. (2008) Phosphatidylinositol 4,5-bisphosphate enhances store-operated calcium entry through hTRPC6 channel in human platelets. *Biochim. Biophys. Acta* **1783,** 84–97
44. Voets, T., Prenen, J., Fleig, A., Vennekens, R., Watanabe, H., Hoenderop, J. G., Bindels, R. J., Droogmans, G., Penner, R., and Nilius, B. (2001) CaT1 and the calcium release-activated calcium channel manifest distinct pore properties. *J. Biol. Chem.* **276,** 47767–47770
45. Schindl, R., Kahr, H., Graz, I., Groschner, K., and Romanin, C. (2002) Store depletion-activated CaT1 currents in rat basophilic leukemia mast cells are inhibited by 2-aminoethoxydiphenyl borate. Evidence for a regulatory component that controls activation of both CaT1 and CRAC (Ca(2+) release-activated Ca(2+) channel) channels. *J. Biol. Chem.* **277,** 26950–26958
46. DeHaven, W. I., Jones, B. F., Petranka, J. G., Smyth, J. T., Tomita, T., Bird, G. S., and Putney, J. W., Jr. (2009) TRPC channels function independently of STIM1 and Orai1. *J. Physiol.* **587,** 2275–2298
47. Huang, G. N., Zeng, W., Kim, J. Y., Yuan, J. P., Han, L., Muallem, S., and Worley, P. F. (2006) STIM1 carboxyl-terminus activates native SOC, I(crac) and TRPC1 channels. *Nat. Cell Biol.* **8,** 1003–1010
48. Alfonso, S., Benito, O., Alicia, S., Angélica, Z., Patricia, G., Diana, K., Vaca, L., and Luis, V. (2008) Regulation of the cellular localization and function of human transient receptor potential channel 1 by other members of the TRPC family. *Cell Calcium* **43,** 375–387
49. Nijenhuis, T., Hoenderop, J. G., van der Kemp, A. W., and Bindels, R. J. (2003) Localization and regulation of the epithelial Ca^{2+} channel TRPV6 in the kidney. *J. Am. Soc. Nephrol.* **14,** 2731–2740
50. Schoeber, J. P., van de Graaf, S. F., Lee, K. P., Wittgen, H. G., Hoenderop, J. G., and Bindels, R. J. (2009) Conditional fast expression and function of multimeric TRPV5 channels using Shield-1. *Am. J. Physiol. Renal Physiol.* **296,** F204–F211
51. Bianco, S. D., Peng, J. B., Takanaga, H., Suzuki, Y., Crescenzi, A., Kos, C. H., Zhuang, L., Freeman, M. R., Gouveia, C. H., Wu, J., Luo, H., Mauro, T., Brown, E. M., and Hediger, M. A. (2007) Marked disturbance of calcium homeostasis in mice with targeted disruption of the Trpv6 calcium channel gene. *J. Bone Miner Res.* **22,** 274–285
52. Xia, Z., and Liu, Y. (2001) Reliable and global measurement of fluorescence resonance energy transfer using fluorescence microscopes. *Biophys. J.* **81,** 2395–2402